THE ASTROPHYSICAL JOURNAL, 416:L41–L44, 1993 October 10

ULTRAVIOLET TRANSITIONS OF LOW CONDENSATION TEMPERATURE HEAVY ELEMENTS AND NEW DATA FOR INTERSTELLAR ARSENIC, SELENIUM, TELLURIUM, AND LEAD[1]

JASON A. CARDELLI,[2] S. R. FEDERMAN,[3] DAVID L. LAMBERT,[4] AND C. E. THEODOSIOU[3]
Received 1993 July 12; accepted 1993 July 28

ABSTRACT

We report on the first interstellar detections of transitions of the heavy elements As II and Se II along with 2 σ upper limits for Te II and Pb II. We also present a line list of the strongest ultraviolet transitions for an additional eight heavy elements, including rest wavelengths and a compilation of existing transition oscillator strengths along with new theoretical values for many species. All these transitions fall within the accessible UV range of the Goddard High Resolution Spectrograph. With two exceptions, all these elements are characterized by relatively low condensation temperatures ($T_c \leq 720$ K) and are therefore expected to be only lightly depleted onto dust. Because these elements are produced by a diverse mixture of slow and rapid neutron capture (*s*- and *r*-process), comparisons involving their measured abundances for different sight lines provide a unique probe of stellar evolution, nucleosynthetic enrichment, and the efficiency with which this material is mixed in the interstellar medium.

Subject headings: atomic data — ISM: abundances — ISM: atoms — techniques: spectroscopic — ultraviolet: interstellar

1. INTRODUCTION

With moderate-resolution (15 km s^{-1}) to high-resolution (3.5 km s^{-1}) gratings and the capability to produce high signal-to-noise ratio (S/N) photon-limited spectra (>100/1), the Goddard High Resolution Spectrograph (GHRS) aboard the *Hubble Space Telescope* (*HST*) has as one of its most significant attributes the ability to produce unprecedented UV data on weak absorption lines (e.g., $W_\lambda < 1$–2 mÅ). For example, the GHRS has been used to obtain data on important abundant species like carbon through the weak intersystem line of C II toward ζ Oph ($W_\lambda = 0.52 \pm 0.12$ mÅ, S/N = 450; Cardelli et al. 1993b). Analysis of weak lines also provides the opportunity to explore moderate to strong transitions of elements with relatively low cosmic abundances [i.e., $\log (N/\mathrm{H})_\odot < -8$]. GHRS observations of ζ Oph have produced new results for low-abundance species including B II and Co II (Federman et al. 1993) and the first measures of the heavier-than-Zn elements Ga II, Ge II, Kr I, and Sn II (Cardelli, Savage, & Ebbets 1991). (We note that the Sn II measurement of Cardelli et al. 1991 was listed as an unidentified line; credit for the first identification of this transition as Sn II goes to Hobbs et al. 1993.) Subsequently, Hobbs et al. (1993) have presented additional measures for Ga II, Ge II, Kr I, and Sn II toward several stars. What makes these heavy elements important is that they arise from nucleosynthetic pathways (*s*- and *r*-process) uniquely different from those that produce Zn and the lighter elements, and thus offer the opportunity to study the effects of nucleosynthetic enrichment and mixing of the interstellar gas.

In this *Letter* we present the first detections of As II and Se II, bringing to six the number of elements heavier than Zn now observed in the interstellar medium (ISM). In addition, we present 2 σ upper limits for the transitions of Te II and Pb II and provide a list of transitions for eight other heavy elements with low condensation temperatures that are likely to be observable with the GHRS.

2. THE DATA

2.1. *Observations*

The results presented here derive from GHRS observations of ζ Oph and were obtained from a combination of science verification and guaranteed time observation programs using the high-resolution (echelle: 3.5 km s^{-1}) and medium-resolution (G160M: 15 km s^{-1}) gratings and the 0.″25 × 0.″25 small science aperture. Each observation was obtained with a substep sampling strategy corresponding to either two (echelle) or four (G160M) samples per science diode width, a four-position comb-addition for reducing diode-to-diode variations, and the procedure FP-SPLIT = 4 (each observation is split into four subexposures, each obtained at a slightly different grating position) for the purpose of assessing and removing the effects of fixed pattern noise and photocathode granularity. The specifics of the general reduction of GHRS data applicable to the observations presented here are discussed in Cardelli et al. (1991), Savage, Cardelli, & Sofia (1992), and Lambert et al. (1994). Wavelengths were assigned from the standard *HST* calibration tables. The final step in the reduction for each individual observation involved correcting for fixed pattern noise/granularity (see Cardelli et al. 1993b), merging the individual FP-SPLIT subexposures, and subtraction of the scattered-light background. This background, which consists of the actual measured background in the interorder above and below the spectral order converted to count rates, is fitted with a low-order polynomial and subtracted from the spectrum. For the echelle data an additional background correction, based on the scattered-light analysis of Cardelli, Ebbets, & Savage (1990, 1993a), was applied.

[1] Based in part on observations obtained with the NASA/ESA *Hubble Space Telescope* through the Space Telescope Science Institute, which is operated by the Association for Research in Astronomy, Inc., under NASA contract NAS 5-26555.
[2] Department of Astronomy, University of Wisconsin–Madison, 475 North Charter Street, Madison, WI 53706.
[3] Department of Physics and Astronomy, University of Toledo, Toledo, OH 43606.
[4] Department of Astronomy, University of Texas, Austin, TX 78712.

2.2. *Heavy-Element Line List*

Although a detailed line list for atomic transitions in the UV applicable to the ISM is available for H through Ge (Morton 1991), no such listing currently exists for heavier elements. A major distinction between these heavy elements and all but six (Li, Be, B, Sc, Ga, and Ge) of the 32 lighter elements is that their measured cosmic abundances (Anders & Grevesse 1989) are extremely low (i.e., less than 1 atom per 10^8–10^9 H atoms) and are therefore expected to produce at best only very weak resonance absorption lines (less than a few mÅ). However, given the capabilities of the GHRS to produce high-quality weak-line data, a heavy-element resonance line list is needed.

In generating a usable line list (Table 1), we considered species that have resonance transitions accessible to the GHRS (e.g., 1150–3100 Å) from ionization states that are expected to dominate under typical ISM conditions (i.e., ionization potential [IP] $\geq$13.6 eV). An exception is Xe I (IP = 12.127 eV), but since its IP is close to that of hydrogen, Xe I may dominate in moderately dense, cold clouds. The observability of a species is a function of the elemental abundance, the transition f-value, and the degree to which the element is depleted onto dust which is reflected by the element's condensation temperature, T_c. With one exception (As), we restricted our list to elements with $T_c \leq 900$ K, since for sight lines like that to ζ Oph, such species are typically depleted by a factor ≤ 3 (Savage et al. 1992; Federman et al. 1993). We have not included species where the strongest line is expected to yield $W_\lambda < 0.1$ mÅ toward a sight line like that to ζ Oph. For example, we have not included Bi II λ1436.83 [$\log (N/\mathrm{H})_m = -11.3$, $T_c = 451$ K, $f \approx 0.25$], since we expect $W_\lambda \approx 0.03$ mÅ. Similarly, I II λ1178.55 [$\log (N/\mathrm{H})_m = -10.5$, $T_c < 600$ K, $f \approx 0.010$] is not included, since we expect $W_\lambda \approx 0.006$ mÅ.

TABLE 1

HEAVY-ELEMENT UV RESONANCE TRANSITION[a]

Species	Z[b]	A_m[c]	T_c[d]	λ (Å)[e]	f-value[ref. code][f]
As II	33	-9.63	1157	1263.77*	**0.32**[T1], 0.18[T2], 0.292[T3], 0.21[T4]
				1181.51	...
				1355.93	...
				1207.44	0.023[T2], 0.016[T3], 0.012[T4]
Se II	34	-8.65	684	1192.29*	...
				1168.53	...
				1156.91	...
Kr I	36	-8.77	~0	1235.83*	0.187[E1], 0.214[E2]
				1164.86*	0.193[E1], 0.193[E2]
Cd II	48	-10.24	430	2145.07	**0.51**[T1], 0.46[E3], 0.40[E4], 0.52[E5]
				2265.72	**0.24**[T1], 0.21[E3], 0.19[E4], 0.25[E5]
In II	49	-11.18	456	1586.45	1.62[T5], 1.48[T6], 1.26[E6], 1.43[E7]
Sn II	50	-9.86	720	1400.44*	**0.64**[T1], 0.80[T7], 1.09[E8]
				1757.90	**0.12**[T1], 0.14[T7], 0.15[E8], 0.15[T8]
Sb II	51	-10.96	912	1438.11	**0.22**[T1], 0.18[T2], 0.234[T3], 0.22[T4]
Te II	52	-9.76	680	1404.63	...
				1335.22	...
Xe I	54	-9.77	~0	1469.60	0.214[E9], 0.273[E2]
				1295.58	0.180[E9], 0.186[E2], 0.194[E1]
Hg II	80	-10.91	<600	1649.95	**0.50**[T1], 0.52[E4], 0.56[E10], 0.44[E11]
				1942.28	**0.22**[T1], 0.21[E4], 0.24[E10], 0.22[E12]
Tl II	81	-11.18	428	1321.70	1.36[T9], 1.36[T10], 1.21[E6]
Pb II	82	-9.95	496	1433.90	**0.86**[T1], 0.87[T7]
				1682.15	**0.13**[T1], 0.14[T7], 0.19[T8]

a Strongest transitions for species with low condensation temperatures likely to be observable in the wavelength range accessible with the GHRS. All species correspond to IP > 13.6 eV except Xe I (IP = 12.127 eV; see text).

b Atomic (proton) number.

c Meteoritic abundance, $\log (\mathrm{X/H})_m$, from Anders & Grevesse 1989.

d Condensation temperature from Wasson 1985.

e Vacuum rest wavelength in angstroms (Å). Transitions indicated with an asterisk have been observed with the GHRS.

f The superscript gives the reference code: T ≡ theoretical, E ≡ experimental. Theoretical: (1) This *Letter* (boldface entries); (2) Gruzdev 1968; (3) Warner & Kirkpatrick 1969; (4) Bieron et al. 1991; (5) Hibbert 1982; (6) Migdalek & Baylis 1986b; (7) Migdalek 1976; (8) Kunisz & Migdalek 1974; (9) Migdalek & Baylis 1986a; (10) Beck & Ziyong 1990. Experimental: (1) Griffen & Hutchenson 1969; (2) Chan et al. 1992; (3) Migdalek & Baylis 1979 using Andersen et al. 1976; (4) Migdalek & Baylis 1979 using Andersen & Sorensen 1973; (5) Hamel & Barrat 1974; (6) Andersen et al. 1972; (7) Ansbacher et al. 1986; (8) Andersen & Lindgard 1977; (9) Wieme & Mortier 1973; (10) Dworetsky 1980; (11) Eriksen & Poulson 1980; (12) Leckrone et al. 1991 using Itano et al. 1987.

The transitions marked with an asterisk in Table 1 represent lines that have been detected with the GHRS, including previously published data (Kr I and Sn II) and new data presented here (As II and Se II). The other transitions were identified by matching analogous transitions among species within a given column (element group) in the periodic table. The rest wavelengths were derived from atomic energy levels (Moore 1971) and are expected to be accurate to ± 0.01 Å in most cases. We performed an extensive search of the literature for absorption oscillator strengths (f-values), and these data are listed in the table. For several species, additional values are available and can be found in tabulations in the cited references, especially those that are more recent. We make no attempt here to assess the relative merits of any specific literature value, opting more for a general compilation. However, the relative agreement between values from different sources is generally quite good, suggesting uncertainties of perhaps $\leq$30%. For the transitions of Kr I, Cd II, Xe I, and Hg II, the experimental data are of sufficient number and quality that weighted mean values from the data in Table 1 are probably accurate to 10%–15%. The significance of f-value uncertainties is discussed further in § 3.2.

The f-values in boldface type in Table 1 are new theoretical values produced by us and were calculated using the Coulomb approximation with a Hartree-Slater core (CAHS). For Cd and Hg the calculations also include core polarization effects. Details of the methodology can be found in Theodosiou (1984a, b).

For the data in Table 1, we have not considered the effects of either hyperfine splitting or isotope shifts. For most heavy elements, we expect these shifts to be relatively small ($\leq$a few km s^{-1}), as is the case for Pb II λ1682, where the measured shift between ^{206}Pb and ^{208}Pb (Bouazza, Guern, & Bauche 1986) is $\Delta\lambda \approx 0.003$ Å (0.5 km s^{-1}). However, for some elements these shifts can be large, as in the case of Hg II λ1942, where 11 hyperfine and isotopic components are present (Leckrone, Wahlgren, & Johansson 1991), corresponding to $\Delta\lambda \approx 0.07$ Å (10 km s^{-1}). In such cases, the presence of these shifts must be considered in assessing the total measured abundance of these species.

3. DISCUSSION

3.1. *New Detections and Upper Limits*

Spectra of the first detections of the transitions of As II λ1264 (ζ Oph) and Se II λ1192 (ξ Per) are shown in Figure 1 along

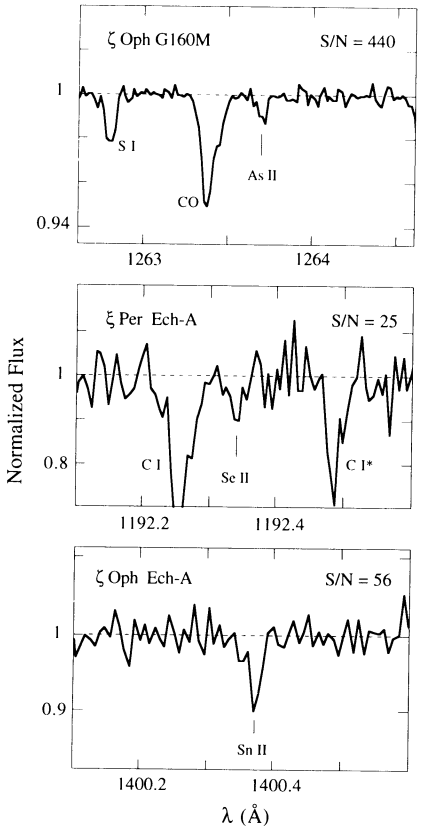

FIG. 1.—Spectra of the observed transitions of As II λ1263.77 (ζ Oph), Se II λ1192.29 (ξ Per), and Sn II λ1400.44 (ζ Oph). Also indicated in the figure are the specific gratings that were used (G160M and Ech-A with 15 and 3.5 km s^{-1} resolution, respectively) and the measured continuum signal-to-noise ratio.

with the profile for Sn II λ1400 observed toward ζ Oph. The GHRS gratings that were used to obtain the data and the measured continuum S/N are indicated on the figure. These detections were within 0.01 Å of their expected wavelengths. Measured equivalent widths along with 1 σ errors are listed in Table 2 for the data in Figure 1. In addition, we list 2 σ upper limits for Sn II λ1400 toward ξ Per and As II λ1356, Te II λ1335, and Pb II λ1682 toward ζ Oph. Also given are the adopted values of the logarithm of the product of the f-value and the rest wavelength from Table 1 (log $f\lambda$), the logarithm of the observed abundance [computed column density normalized to hydrogen, log (X/H)], and the observed abundance normalized to the meteoritic abundance [$A_{X/H} \equiv$ log (X/H) − log $(X/H)_m$] from Anders & Grevesse (1989). All the lines are weak enough that column densities (cm^{-2}) were derived from the weak-line limit $N(X) = 1.13 \times 10^{20} W_\lambda / f\lambda^2$.

3.2. *Interstellar Heavy-Element Abundances: Significance and Pitfalls*

The new detections of As II and Se II bring to six the number of heavier-than-Zn elements (Ga, Ge, As, Se, Kr, and Sn) now detected in the ISM. These elements ($Z > 30$) are useful to study because their nucleosynthetic origins differ from those of the lighter elements ($Z \leq 30$) traditionally studied in the ISM of which S and Zn are prominent for their low T_c. The processes contributing to the formation of the heavy elements listed in Table 1 are shown graphically in Figure 2 (Cameron 1982a, b) and consist of a diverse mixture of slow and rapid neutron capture (s- and r-process). In the usual assignment of the heavy elements to neutron capture processes (Kappeler, Beer, & Wisshak 1989), the s-process primarily responsible for Ge to Kr is a mild exposure believed to occur in hydrostatic burning of massive stars (the "weak" s-process). The s-process contributing the heavier elements (Rb to Pb) is termed the main s-process and is widely supposed to occur in the He shells of asymptotic giant branch (AGB) stars. A third s-process ("strong" component) has been introduced to account for the meteoritic abundance of ^{208}Pb at the termination of the s-process path. Gallino et al. (1990) suggest that the site of this component is the He shell of low-mass metal-poor AGB stars.

Intercomparison of measured abundances of elements arising from a range of formation mechanisms within and between different sight lines provides a unique probe of stellar evolution, nucleosynthetic enrichment, and the efficiency with which this material is fixed in the ISM. For example, intra–sight-line abundance comparisons between Se, Kr, Sn, Hg (75%–80% s-process) and Sb, Te, Xe (75%–85% r-process) can provide a useful probe of s-process/r-process contributions, while comparisons within these two groups can serve as a check of the predicted s- and r-process contributions. Com-

TABLE 2

NEW HEAVY-ELEMENT DETECTIONS AND UPPER LIMITS[a]

Species	λ (Å)	log $f\lambda$[b]	W_λ (±1 σ)[c]	Grating	S/N[d]	log (X/H) (±1 σ)[e]	$A_{X/H}$[f]
As II	1263.77	2.50	0.68 (0.16)	G160M	440	−9.87 (0.09)	−0.24
	1355.93	1.73[g]	<0.4 (2 σ)		360	< −9.35 (2 σ)	< +0.28
Se II	1192.29	1.55[g]	2.25 (1.23)[h]	Ech-A	25	−8.51 (0.23)	+0.13
Sn II	1400.44	3.00	2.69 (0.54)	Ech-A	56	−9.81 (0.09)	+0.05
			<2 (2 σ)[h]		35	< −10.08 (2 σ)	< −0.22
Te II	1335.22	1.43[g]	<0.5 (2 σ)	G160M	320	< −8.96 (2 σ)	< +0.80
Pb II	1682.15	2.42	<0.8 (2 σ)	G160M	230	< −9.84 (2 σ)	< +0.11

[a] Data obtained for the sight line to ζ Oph, log $N(H_{total}) = 21.15$, except where noted.
[b] Logarithm of the product of the mean f-value and rest wavelength. For Sn II we used an average of the theoretical values, since the experimental value was calculated from the measured multiplet lifetime assuming LS coupling, which may not be appropriate for very heavy elements.
[c] Measured equivalent width and 1 σ error in milliangstroms (mÅ).
[d] Measured continuum signal-to-noise ratio.
[e] Logarithm of the measured column density relative to hydrogen and 1 σ error.
[f] Normalized abundance of species X, $A_{X/H} \equiv$ log (X/H) − log $(X/H)_m$.
[g] f-values adopted from the mean values of the isoelectronic sequence for elements with homologous transitions.
[h] Data obtained for the sight line to ξ Per, log $N(H_{total}) = 21.29$.

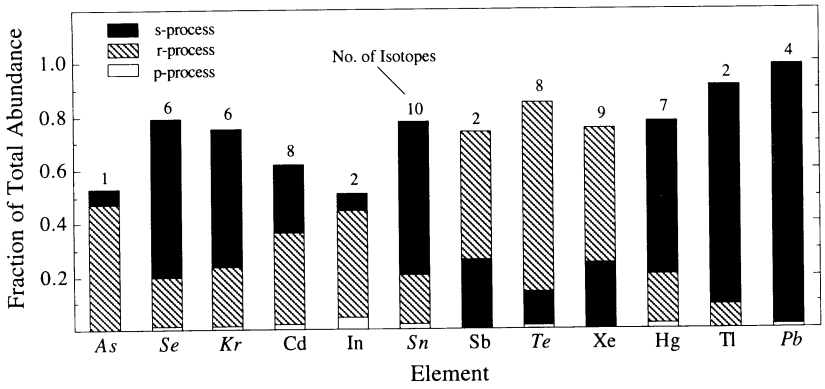

FIG. 2.—Processes responsible for the formation of the heavy elements listed in Table 1 in terms of their relative fractional contributions. These data were derived from the compilations of Cameron (1982a, b). The italicized species represent elements that have been detected with the GHRS, except for Te and Pb, for which we only have an upper limit. Also indicated is the number of isotopes for each element.

parison of the relative abundances among different isotopes of the same element (e.g., Hg) can also provide useful probes of predicted contributions from stellar evolution theory.

There are several pitfalls associated with interpreting measured interstellar gas-phase abundances. One involves uncertainties in adopted f-values which directly translate to uncertainties in the absolute elemental abundances (e.g., As/H) or their intercomparison in single sight lines. However, in probing variations of abundances or abundance ratios *between different sight lines*, f-value uncertainties do not apply. In fact, one does not even need f-values in such cases, provided that the lines are in the weak-line limit. We expect this to be the case for all the species listed in Table 1. Another pitfall involves depletion onto dust, which is generally a function of the element's condensation temperature (Wasson 1985, p. 250), with larger depletions occurring for larger values of T_c (Jenkins 1987). However, for elements with $T_c \leq 900$ K, depletions are relatively small (a factor of ≤ 3), even in cold, dense clouds like ζ Oph (Savage et al. 1992; Federman et al. 1993). Furthermore, Jenkins (1987) and Joseph (1988) have shown that when the depletion of one element changes (increases or decreases), all elements exhibit proportional changes *in the same direction*. Thus, intercomparison of abundance ratios *between different sight lines*, especially between elements with similar bulk depletion characteristics, provides a nucleosynthetic probe relatively free of depletion effects. Of particular interest in this regard are Ar (100% O, Si burning), Kr (76% s-process), and Xe (75% r-process). Since these species are not expected to react with dust in their neutral state (Cardelli et al. 1991), their measured abundances are a direct probe of the cosmic abundance. Some literature data exist for Ar I and Kr I. From the data in Table 1 we expect $W_\lambda \approx 1$ mÅ for Xe I λ1469 toward ζ Oph, assuming Xe I is the dominant state. Finally, analyses of isotopic ratios for the same element are free of the pitfalls associated with uncertainties in f-values and depletion, even in single sight lines.

We gratefully acknowledge assistance from and useful discussions with Jim Lawler, Francis Keenan, and Roberto Gallino. J. A. C. acknowledges support from NASA-LTSARP grant NAGW-2520. D. L. L. acknowledges support from NASA grant NAG 5-1616.

REFERENCES

Anders, E., & Grevesse, N. 1989, Geochim. Cosmochim. Acta, 53, 197
Andersen, T., Kirkegard Nielsen, A., & Sorensen, G. 1972, Phys. Scripta, 6, 122
Andersen, T., & Lindgrad, A. 1977, J. Phys. B, 10, 2359
Andersen, T., Poulsen, O., & Ramanujam, P. S. 1976, J. Quant. Spectrosc. Rad. Transf., 13, 369
Andersen, T., & Sorensen, G. 1973, J. Quant. Spectros. Rad. Transf., 16, 521
Ansbacher, W., Pinnington, E. H., Kernahan, J. A., & Gossenlin, R. N. 1986, Canadian J. Phys., 64, 1365
Beck, D. R., & Ziyong, C. 1990, Phys. Rev. A, 41, 301
Bieron, J. R., Marcinek, R., & Migdalek, J. 1991, J. Phys. B, 24, 31
Bouazza, S., Guern, Y., & Bauche, J. 1986, J. Phys. B, 19, 1881
Cameron, A. G. W. 1982a, Ap&SS, 82, 123
———. 1982b, Essays in Nuclear Astrophysics (Cambridge: Cambridge Univ. Press), 23
Cardelli, J. A., Ebbets, D. C., & Savage, B. D. 1990, ApJ, 365, 789
———. 1993a, ApJ, 413, 401
Cardelli, J. A., Mathis, J. S., Ebbets, D. C., & Savage, B. D. 1993b, ApJ, 402, L17
Cardelli, J. A., Savage, B. D., & Ebbets, D. C. 1991, ApJ, 383, L23
Chan, W. F., Cooper, G., Guo, X., Burton, G. R., & Brion, C. E. 1992, Phys. Rev. A, 46, 149
Dworetsky, M. M. 1980, A&A, 84, 350
Eriksen, P., & Poulsen, O. 1980, J. Quant. Spectros. Rad. Transf., 23, 599
Federman, S. R., Sheffer, Y., Lambert, D. L., & Gilliland, R. L. 1993, ApJ, 413, L51
Gallino, R., Busso, M., Picchio, G., & Raiteri, C. M. 1990, in Chemical and Dynamical Evolution of Galaxies, ed. F. Ferrini, J. Franco, & F. Matteucci (Pisa: ETS Editrice), 338
Griffen, P. M., & Hutchenson, J. W. 1969, J. Opt. Soc. Am., 59, 1607
Gruzdev, P. F. 1968, Opt Spectrosc., 25, 1
Hamel, J., & Barrat, J.-P. 1974, Opt. Comm., 10, 331
Hibbert, A. 1982, Nucl. Instr. Meth., 202, 323
Hobbs, L. M., Welty, D. E., Morton, D. C., Spitzer, L., & York, D. G. 1993, ApJ, 411, 750
Itano, W. M., Bergquist, J. C., Hulet, R. G., & Wineland, D. J. 1987, Phys. Rev. Lett., 59, 2732
Jenkins, E. B. 1987, in Interstellar Processes, ed. D. J. Hollenbach & H. A. Thronson (Dordrecht: Reidel)
Joseph, C. L. 1988, ApJ, 335, 157
Kappeler, F., Beer, H., & Wisshak, K. 1989, Rep. Progr., Phys., 52, 945
Kunisz, M. D., & Migdalek, J. 1974, Acta Phys. Polonicae, A45, 715
Lambert, D. L., Sheffer, Y., Gilliland, R. L., & Federman, S. R. 1994, ApJ, in press
Leckrone, D. S., Wahlgren, G. M., & Johansson, S. G. 1991, ApJ, 377, L37
Migdalek, J. 1976, J. Quant. Spectrosc. Rad. Transf., 16, 265
Migdalek, J., & Baylis, W. E. 1979, J. Quant. Spectrosc. Rad. Transf., 22, 113
———. 1986a, J. Phys. B, 18, 1533
———. 1986b, J. Phys. B, 19, 1
Moore, C. E. 1971, Atomic Energy Levels (NSRDS-NBS), 35
Morton, D. C. 1991, ApJS, 77, 119
Savage, B. D., Cardelli, J. A., & Sofia, U. J. 1992, ApJ, 401, 706
Theodosiou, C. E. 1984a, Phys. Rev. A, 30, 2881
———. 1984b, Phys. Rev. A, 30, 2910
Warner, B., & Kirkpatrick, R. C. 1969, MNRAS, 142, 265
Wasson, J. T. 1985, Meteorites: Their Record of the Early Solar System History (New York: Freeman)
Wieme, W., & Mortier, P. 1973, Physica, 65, 203